

SUPPLEMENTAL MATERIAL

The Phosphoenolpyruvate: Sugar Phosphotransferase system is involved in sensitivity to the glucosylated bacteriocin sublancin

C. V. Garcia De Gonzalo^{1*}, E. L. Denham^{2,3*}, R. A. T. Mars^{3a}, J. Stülke⁴, W. A. van der Donk¹, and J. M. van Dijl³

*Equal contribution

1 - Howard Hughes Medical Institute and Roger Adams Laboratory, Department of Chemistry, University of Illinois at Urbana-Champaign, 600 South Mathews Avenue, Urbana, Illinois 61801, United States

2 - Division of Translational and Systems Medicine, Unit of Microbiology and Infection, Warwick Medical School, University of Warwick, Coventry, CV4 7AL, UK

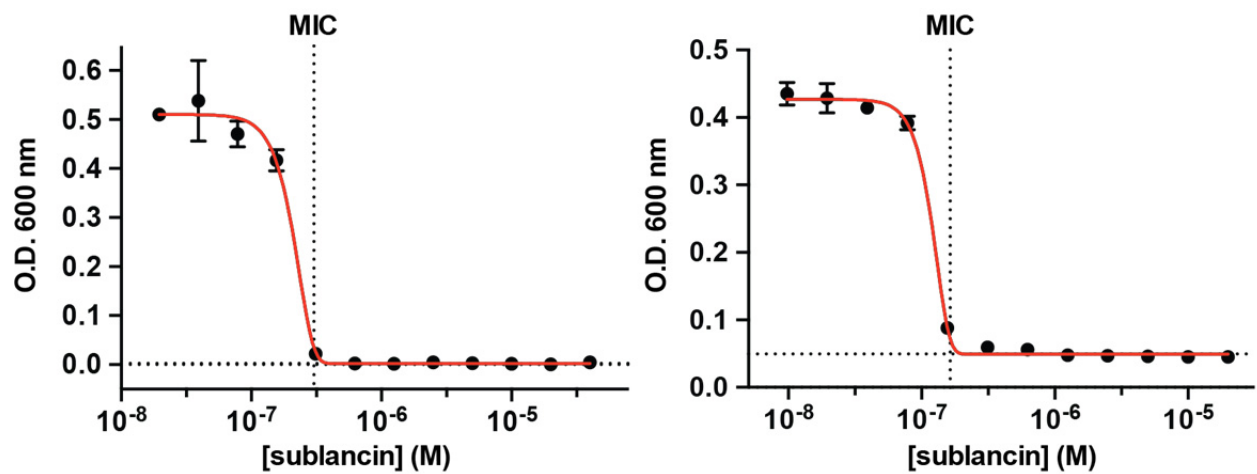
3 - Department of Medical Microbiology, University Medical Center Groningen and University of Groningen, Hanzeplein 1, 9700 RB Groningen, the Netherlands

a - Current Address

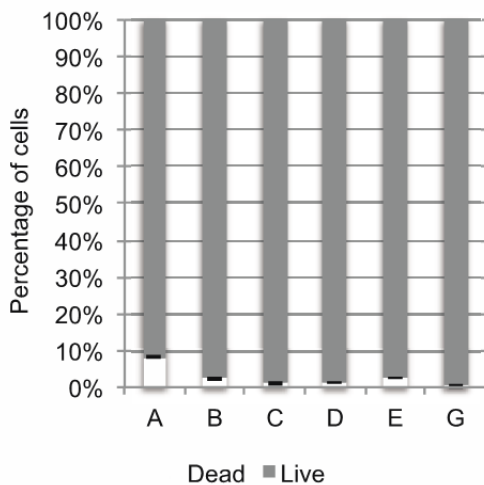
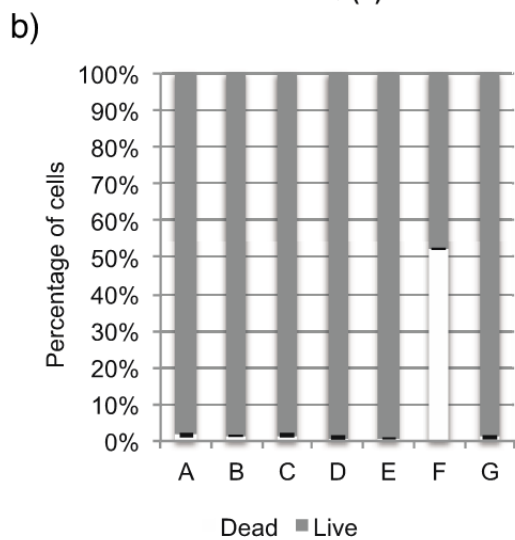
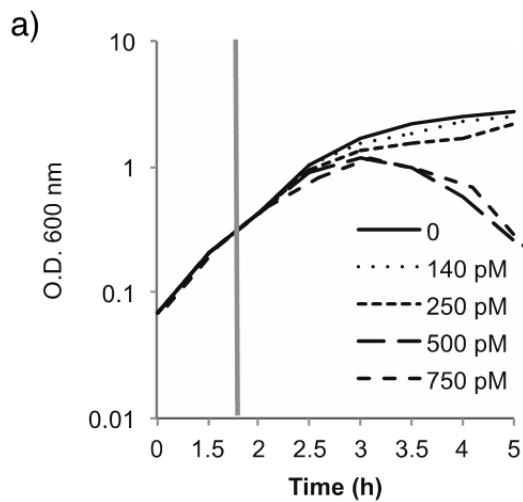
Institute of Molecular Systems Biology, ETH Zürich, Auguste-Piccard-Hof 1, 8093 Zürich, Switzerland

4 - Institut für Mikrobiologie und Genetik, Abteilung für Allgemeine Mikrobiologie, Grisebachstr. 8, 37077 Göttingen, Germany

Supplementary Figures and Tables



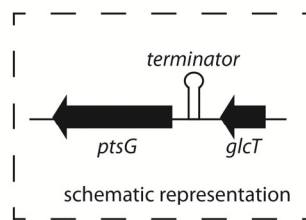
Supplementary figure S1. Determination of the specific activity of sublancin against *Bacillus subtilis* ATCC 6633 (left) and *Bacillus halodurans* C-125 (right) by the broth dilution method. Shown are the means of a single experiment conducted in triplicate as a representative of three independent experiments. For both graphs $R^2 > 0.99$. Error bars indicate standard deviations.



Supplementary figure S2. Sublancin does not affect the integrity of the bacterial membrane. (a) Growth curve of the *B. subtilis* $\Delta SP\beta$ strain in the presence of different concentrations of sublancin. Sublancin was added at O.D._{600nm} 0.5 (vertical grey line). Measurements were performed in a Synergy 4 plate reader every 10 min in triplicate and the means of the growth curve was plotted. (b) LIVE/DEAD® *BacLight*™ bacterial cell viability assay of the $\Delta SP\beta$ strain 30 (top) and 90 (bottom) min after exposure to sublancin.

Grey bars depict bacteria with an intact membrane and white bars depict bacteria with a compromised membrane, error bars depict standard deviation of triplicate experiments. A: 100 nM sublancin, B: 200 nM sublancin, C: 300 nM sublancin, D: 400 nM sublancin, E 500 nM sublancin, F Nisin (10 nM) was used as a positive control that does affect the integrity of the membrane, G negative control, no addition of an antimicrobial agent.

wild type *B. halodurans* C-125
 Predicted terminator



Calculated wild type terminator
 $\Delta G = -44.6$ kcal/mol

919995 | GAAGAAAACCUCCUUUGAUGUUACAACCGAAAAAAUCACACAACAAAAA:UGCAUAACCGUAACACGGAAACAAAAUUGCCAG | 920169

resistant mutant *B. halodurans* C-125
 Predicted terminator

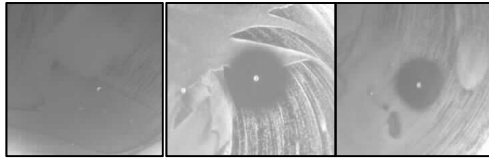


Calculated mutant terminator
 $\Delta G = -56.5$ kcal/mol

919995 | GAAGAAAACCUCCUUUGAUGUUACAACCGAAAAAAUCACACAACAAAAA:UGCAUAACCGUAACACGGAAACAAAAUUGCCAG | 920169

Supplementary figure S3. Predicted secondary structures of the terminator of (top) wild-type *B. halodurans* C-125 (accession no. NC_002570.2) and (bottom) the sublancin resistant mutant *ptsG* leader mRNA. Inset shows a schematic representation of the genomic locus. Terminators are shown in the antisense strand since flanking genes translate in an antisense fashion. The terminator starts at position 920136 and ends at position 920046. The *ptsG* starts at position 919994. Single nucleotide polymorphisms (SNPs) are labelled in red, and the location in the genome is shown. The RNAstructure Web Server (<http://rna.urmc.rochester.edu/RNAstructureWeb/index.html>) at the University of Rochester Medical Center and the RNAfold Web Server (<http://rna.tbi.univie.ac.at/>) at

the University of Vienna were used to predict the secondary structures using default parameters. All three mutations result in Watson-Crick base-paired bases that increase the strength of the terminator. The predicted free energy values for the terminator loops were calculated using the RNAstructure Web Server.



M9-Glucose

M9-
Citrate

M9-
Malate

Supplementary figure S4. *B. subtilis* Δ SPB was spread over M9 agar plates containing 0.3% glucose, 0.4% citrate or 0.4% malate. Sublancin (2 μ L of 100 nM) was spotted on the plates. The presence of glucose in the media resulted in resistance to sublancin.

yvkS-ykvWP1	ttctacacgaggcattacatt
yvkS-ykvWP2	CGACCTGCAGGCATGCAAGCTcccttttcttctattgacga
yvkS-ykvWP3	CGAGCTCGAATTCACCTGGCCGTCGaggctgctggccttttat
yvkS-ykvWP4	cacatgggtttcttcattt
ykvY-glcTP1	cttgataaaaccggaactg
ykvY-glcTP2	CGACCTGCAGGCATGCAAGCTtgttctcctgccattt
ykvY-glcTP3	CGAGCTCGAATTCACCTGGCCGTCGattcagttatcctataacgtg
ykvY-glcTP4	gtgtttgatgtttcctggt
ptsG-ptsIP1	ctacaaagaggcattggaag
ptsG-ptsIP2	CGACCTGCAGGCATGCAAGCTaagaattgacctcctctttt
ptsG-ptsIP3	CGAGCTCGAATTCACCTGGCCGTCGtaacatggctaggaggata
ptsG-ptsIP4	aggaaaaacgacctgtg

Supplementary table S1. Oligonucleotides used in this study to generate deletion mutants described in Table 2. Capital letters indicate overlapping regions with phleomycin resistance cassette, lower case letters indicate regions complementary to *B. subtilis* genome.

Nucleotide position	Locus tag	Genetic component	Frequency	SNP mutation
919515	BH0844	PTS system glucose-specific transporter subunit IIC	3/4	G → T
920055	Between	Intergenic region between	1/4	G → A
920075	BH0844	transcriptional antiterminator		C → T
920079	BH0845	and PTS system glucose-specific enzyme II, ABC components		A → G
3977494	BH3851	Mannitol-1-phosphate 5-dehydrogenase	1/4	T → C

Supplementary table S2. SNPs in genes of sublancin-resistant *B. halodurans* C-125 mutants determined by Illumina sequencing. The mutation in BH0844 results in a stop codon instead of a Tyr codon at position 160. The predicted domain organization of PtsG of *B. halodurans* C-125 is: 1-424 domain IIC, 425-524 domain IIB, and 525-675 domain IIA (see schematic drawing of the predicted domain organization in Supplementary table S4). Hence, the stop codon would delete most of PtsG and the respective truncated product would likely not be expressed as a stable protein. The mutation in BH3851 results in a His to Arg mutation. As shown in Supplementary figure 3, the mutations in the intergenic region result in a change in the predicted antiterminator structure that may affect transcription of *ptsG*.

Category and Locus Tag	Entrez Gene ID	Gene	Name	Fold Change in transcript level
Sulfur metabolism				
BH1487	890521	<i>sat</i>	Sulfate adenylyltransferase	16
BH1486	890994	<i>cysH</i>	3'-phosphoadenosine 5'-phosphosulfate reductase	14
BH0088	891637	<i>cysK</i>	cysteine synthase A	11
BH1489	890544	NA	adenylylsulfate kinase	9
Transmembrane transporter activity				
BH1488	890630	NA	sodium-dependent phosphate transporter	12
BH3129	890493	<i>cysW</i>	sulfate ABC transporter (permease)	7
BH3128	890497	<i>cysT</i>	sulfate ABC transporter (permease)	5
BH3127	894370	NA	sulfate ABC transporter (sulfate-binding protein)	5
BH3130	890510	<i>cysA</i>	sulfate ABC transporter (ATP-binding protein)	5
Amino sugar and nucleotide sugar metabolism				
BH0421	892066	<i>nagA</i>	N-acetylglucosamine-6-phosphate deacetylase	9
BH3130	894561	<i>nagB</i>	N-acetylglucosamine-6-phosphate isomerase	5
BH0675	893039	NA	beta-hexosamidase A precursor	5
BH1086	894063	<i>glgD</i>	required for glycogen biosynthesis	4
BH1087	892001	<i>glgC</i>	glucose-1-phosphate adenylyltransferase	4
BH0422	893420	NA	PTS system, N-acetylglucosamine-specific enzyme II, ABC component	3
BH1874	892569	XSA	alpha-L-arabinosidase	3
<i>Continued on next page</i>				

Category and Locus Tag	Entrez Gene ID	Gene	Name	Fold Change in transcript level
BH0673	893046	NA	PTS system, n-acetylglucosamine-specific enzyme II, ABC component (EIIABC-Nag)	2
BH3784	894582	<i>murZ</i>	UDP-N-acetylglucosamine 1-carboxyvinyltransferase	-2
BH0065	892269	<i>gcaD</i>	UDP-N-acetylglucosamine pyrophosphorylase	-2
BH2564	894513	<i>murB</i>	UDP-N-acetylenolpyruvoylglucosamine reductase	-2
BH0797	892380	NA	Glucose kinase	-2
BH0267	894435	NA	phosphoglucosamine mutase	-3
BH0844	892408	<i>ptsG</i>	PTS system, glucose-specific enzyme II, ABC component	-4
BH3715	894300	NA	UDP-glucose 4-epimerase	-6
BH3343	891275	<i>pgi</i>	glucose-6-phosphate isomerase	-8
BH3074	890548	<i>ptsH</i>	PTS system, histidine-containing phosphocarrier protein (HPr)	-8
BH1515	890569	<i>ypqE*</i>	PTS system, glucose-specific enzyme II, A component	-9
<p>* Closest homolog in <i>B. subtilis</i> is a IIA stand-alone domain <i>YpqE</i> with unknown specificity. NA: specific gene name not available for <i>B. halodurans</i> C-125.</p>				

Supplementary table S3. Changes in transcript levels in *B. halodurans* C-125 in response to the addition of sublancin. Positive numbers indicate up-regulated transcripts, negative numbers indicate down-regulated transcripts.

Begin	End	Length	Localization
1	11	11	Inside
12	32	21	Membrane
33	43	11	Outside
44	60	17	Membrane
61	66	6	Inside
67	83	17	Membrane
84	88	5	Outside
89	109	21	Membrane
110	120	11	Inside
121	149	29	Membrane
150	168	19	Outside
169	189	21	Membrane
190	209	20	Inside
210	232	23	Membrane
233	276	44	Outside
277	295	19	Membrane
296	301	6	Inside
302	319	18	Membrane
320	324	5	Outside
325	349	25	Membrane
350	355	6	Inside
356	373	18	Membrane
374	378	5	Outside
379	401	23	Membrane
402	675	274	Inside

Supplementary table S4. Predicted topology of PtsG from *B. halodurans* C-125 (BH0844). The multidomain PtsG is 675 amino acids in length. PtsG IIC (region 1-424) is a transmembrane domain. PtsG IIB (region 425-524) and PtsG IIA (region 525-675) are cytoplasmic domains. Prediction obtained from the CAMPS (Computational Analysis of the Membrane Protein Space) database (identifiers: Q9KEK8_BACHD, GI:15613407).

